行政院國家科學委員會專題研究計畫　期中進度報告

大夫涅耳數值的微晶片雷射之時空動力研究(1/2)

計畫類別：個別型計畫
計畫編號：NSC91-2112-M-009-030-
執行期間：91年08月01日至92年07月31日
執行單位：國立交通大學電子物理學系

計畫主持人：陳永富

報告類型：精簡報告

處理方式：本計畫可公開查詢

中　華　民　國 92年5月13日

行政院國家科學委員會補助專題研究計畫成果報告

※※※※※※※※※※※※※※※※※※※※※※※※

※※※

※

※　大夫涅耳數值的微晶片雷射之時空動力研究（1/2）

※

※

※

※※※※※※※※※※※※※※※※※※※※※※※※

※※

計畫類別：■個別型計畫　　□整合型計畫

計畫編號：NSC 91－2112－M－009－030－

執行期間：91 年 8月 1 日至 92 年 7 月 31 日

計畫主持人：陳 永 富　教授

共同主持人：

本成果報告包括以下應繳交之附件：

□赴國外出差或研習心得報告一份

□赴大陸地區出差或研習心得報告一份

□出席國際學術會議心得報告及發表之論文各一份

□國際合作研究計畫國外研究報告書一份

執行單位：國立交通大學電子物理系

中　華　民　國　92 年　5　月　12　日

行政院國家科學委員會專題研究計畫成果報告

大夫涅耳數值的微晶片雷射之時空動力研究（1/2）

Spatiotemporal dynamics in a large-Fresnel-number microchip laser

計畫編號：NSC 91－2112－M－009－030－

執行期限：91 年 8月 1 日至 92 年 7 月 31 日

主持人：陳永富　交通大學電子物理系

一、中文摘要

本計畫研究大夫涅耳數值的微晶片雷射中橫模形態動力學。其中的主題包括(1) 激發分布的影響(doughnut shape versus top hat)，(2) 橫模形態與共振腔腔內 Q 因子(cavity Q-value)的關係，(3) 橫模的頻率間距(transverse mode spacing)對形態的時空動力之影響(spatio-temporal dynamics)。

關鍵詞：雷射、橫模形態、形態發生學、時空動力學、光學旋渦

Abstract

A transition from a pure Laguerre-Gaussian (LG) mode to a pattern of optical vortex lattices in a large-Fresnel-number microchip laser is experimentally demonstrated by controlling the cavity Q-factor. The cooperative frequency-locking of nearly degenerate modes is found to be a primary process for the generation of the optical vortex lattices in a class-B laser. When the cavity Q-factor is high enough, a LG-like mode and a structure of optical vortex lattices are found to coexist. Competition between coexisting transverse patterns of different symmetry gives rise to chaotic fluctuations.

Keywords: laser, transverse pattern, pattern formation, spatiotemporal dynamics, optical vortices

二、緣由與目的

Spatiotemporal pattern formations appear spontaneously in a wide range of systems, including hydrodynamics, granular media, chemical reactions, and optics when they are driven sufficiently far from thermodynamic equilibrium [1-4]. In an optical system far from equilibrium, two types of pattern formation have been identified [5]. One is called a pure pattern that can be successfully described in terms of the empty cavity eigenmodes, in the absence of nonlinearities. Nonlinearities imply the interaction of many eigenstates, or pure patterns. The other one is essentially nonlinear pattern formation that generally requires a large Fresnel number of the resonator.

Depending on the material decay constants and photon decay rate, laser media are roughly classified into three type, Class A, B and C. In a Class A laser both the material polarization dephasing and population decay rates are much larger than the photon damping rate and the material variables can be regarded as being slaved to the latter. A Class B laser differs in that the polarization dephasing rate greatly exceeds the photon and population decay rates and hence it is slaved to the other two variables. In a Class C laser, all damping rates are comparable in magnitude. The theoretical investigation for nonlinear pattern formation is generally based on solving the order parameter equation (OPE). The OPE for class-A laser is the complex Swift-Hohenberg equation (CSHE) [6-9], whereas the OPEs for the class-B laser is a CSHE coupled to the slow population equation [10-12]. The numerical integration of CSHE shows that nonzero detuning causes excitation of strip patterns in the one-dimensional (1D) space or of vortex lattices in the 2D case. The vortices are extremely interesting because vortex structure appears so widely in nature-in gases, fluids/superfluids, plasmas, and even in living things, as in the helix of DNA. It is expected that the laser pattern dynamics and dynamics of other distributed nonlinear system have common features. However, it is difficult experimentally to observe the nonlinearity-controlled patterns in laser systems because the requirements comprise both a large Fresnel number of the resonator and a high level of degeneracy of transverse mode families.

The recent rapid progress of diode-pumped microchip lasers has driven a renaissance of solid-state laser physics research and led to novel phenomena [13,14]. The microchip laser can be easily operated in single longitudinal mode more than ten times above threshold before the second longitudinal mode reaches threshold because the gain medium has a short absorption depth that reduces the longitudinal spatial-hole-burning effect [15]. Here we clearly demonstrate the dependence of the transverse pattern formation on the cavity quality factor (Q-factor) in a large-Fresnel-number microchip laser excited by a doughnut pump profile. For increasing the cavity Q-factor, the transverse pattern shows a transition from a pure Laguerre-Gaussian (LG) mode to a nonlinear pattern of square vortex lattices (SVL). The stability of the SVL is found to depend mainly on the transverse mode spacing and the pump power. By further increasing the cavity Q-factor, we find the coexistence of transverse patterns of a LG-like mode and a nonlinear SVL structure. Competition between coexisting transverse patterns of different symmetry gives rise to chaotic fluctuations.

三、結果與討論

The experimental cavity we use is analogous to the one described in Ref. [16]. The system schematic and the pump profile in the laser system are shown in Fig. 1. The gain medium in the experiment is a-cut 2.0 at.% 1 mm length Nd:YVO$_4$ microchip crystal. The absorption coefficient of the Nd:YVO$_4$ crystal is about 6 mm^{-1} at 809 nm. We setup the resonator length to be as short as possible for reaching single-longitudinal mode operation. The total length in the present resonator is L=2.5 mm. The frequency spacing between consecutive longitudinal modes $\Delta\nu_L$ is about 60 GHz. Since the longitudinal-mode spacing is considerably greater than the transverse-mode spacing, the present laser can be easily operated in single longitudinal mode to study the pattern formation. The pump source is a 1 W fiber-coupled laser diode (Coherent, F-81-800C-100) with a 100 μm of core diameter. With a special coupling condition, the output intensity of the fiber-coupled laser diode can be controlled to be like a doughnut distribution. The doughnut pump profile is the key technique in the present investigation of the pattern formation and competition. The pump power was focused into the microchip gain medium by using a focusing lens with 0.57 magnification.

For the general two-mirror resonator, the Fresnel number can be expressed as $Fr = a^2 / \left(\pi\omega_o^2\right)$, where a^2 is the aperture area and $\pi\omega_o^2$ is the area of the lowest-order mode cross. For an end-pumped microchip laser, the effective aperture is usually determined by the pump cross section not by the mirror aperture. Namely, the Fresnel number for an end-pumped microchip laser is given by $Fr = \omega_p^2 / \omega_o^2$, where ω_p is the pump size on the gain medium. Changing the pump-to-mode size ratio ω_p / ω_o can therefore control the value of Fresnel number. For the present cavity, the mode size on the microchip is given by $\omega_o^2 = \left(\lambda\sqrt{L\left(R-L\right)}\right)/\pi$, where L is the cavity length and R is the radius of curvature of the output coupler. Three different output couplers are used in the experiment; the radii of curvature are 200 mm, 50 mm and 10 mm, respectively. For L=2.5 mm, the mode size on the microchip is calculated to be 0.087 mm, 0.061 mm and 0.038 mm, respectively, for R=200 mm, R=50 mm and R=10 mm. Defocusing the pump source, the pump size can be adjusted within 0.5~0.8 mm. The maximum pump size depends on the lasing threshold. Using $\lambda = 1.064$ μm and L=2.5 mm, the Fresnel number can vary from 35 to 85 for R=200 mm. On the other hand, the Fresnel number can be vary from 180 to 440 for R=10 mm. Note that the thermal lensing effect is not significant because the thermal power density on the gain medium is controlled to be less than 0.5 W/mm^2.

First we used an output coupler of R=50 mm with the reflectivity of 97% in the laser resonator. Near lasing threshold, the laser emits a pure high-order LG TEM$_{0,l}$-mode with the distribution $\cos^2 l\phi$ (or $\sin^2 l\phi$) in azimuthal angle, having 2l nodes in azimuth. The laser oscillating on a single high-order LG mode results from a doughnut-shape pump profile. As shown in Fig. 2, the free-running single-transverse-mode class-B laser displays relaxation oscillations that play an important role in the dynamics of multi-transverse-mode class-B lasers. Slightly above lasing threshold, the present laser usually emits a pair of transverse LG TEM$_{0,l}$ cosine and sine modes with chaotic dynamics. A nonlinear system of the Maxwell-Bloch equation [16] has been used to investigate the interaction of two nearly degenerate transverse modes in a class-B laser. It is found that the appearance of dynamic chaos arises from the interaction of the relaxation frequency and the frequency difference between the nearly degenerate modes. The frequency difference between the nearly degenerate modes generally comes from the cross-saturation and other astigmatism.

The cavity-factor Q is defined as $Q = 2\pi \times (\text{energy stored})/(\text{energy lost in one oscillation cycle})$. To excite a continuum of transverse modes simultaneously, we increased the cavity-factor Q by using an output coupler with a higher reflectivity. With an output coupler of R=50 mm with the reflectivity of 99%, we have observed a succession of spatially well-organized SVL patterns (Fig. 2), as predicted in ref. [10]. An optical vortex is a point where the filed intensity is zero and the circulation of the phase gradient on any loop which encloses that point is equal to $2\pi m$ where the integer m is the topological charge of the vortex. As found in ref. [17], the square patterns observed are optical vortices of absolute charge 1. The complexity of the SVL pattern increases with the Fresnel number and its axis along with the orientation of the optical axes of the microchip gain medium. The experimental result confirms the theoretical prediction that the most natural transverse patterns for large-Fresnel-number lasers are the SVLs if transverse-mode families with a high level of degeneracy are excited [6,10]. Nevertheless, it should be noted that all the analytical investigations deal with plane mirrors whereas the experimental result presented uses curved mirrors. The present experiment also provides the first observation of the transition from a linear to an essentially nonlinear pattern formation in a large-Fresnel-number class-B laser. The measurement of the optical spectrum displays that the SVL pattern was a single-mode emission rather than a combination of multimodes. This result indicates that the formation of SVL patterns is a spontaneous process of transverse mode locking of nearly degenerate modes, assisted by the saturation process of the laser nonlinearity. Accompanying the relaxation frequency, the power spectrum of the SVL pattern displays a self-induced oscillation mode, as shown in Fig. 2. The self-induced oscillation mode generally is found to have the same pump-power dependence as the relaxation oscillation. The numerical analysis of the OPEs [10] show that a stable SVL pattern in a large-Fresnel-number class-B laser is in general difficult to exist because inertia of population inversion influences the transverse dynamics. Only when the lasing spectrum range is less than the relaxation oscillation frequency, a stable SVL pattern with self-induced oscillations can be found in a class-B laser. This situation is consistent with the experimental result that the cooperative frequency locking of nearly degenerate modes is an essential process of finding the self-induced oscillation accompanied by the relaxation oscillation in the SVL pattern. Although similar transverse mode locking in the generation of optical vortex crystals was demonstrated in broad-area VCSELs [17], optical systems so far have not generated such a large number of vortices.

The transverse mode spacing $\Delta\nu_T$ governs the coupling strength between the transverse modes and thus rules the influence of the nonlinearity on the dynamical behavior. The theoretical analysis of the OPEs indicate that when the reduced pump parameter ε exceeds the critical value $C\,\Delta\nu_T/\kappa$, a chaotic regime could appear and the vortices in the square pattern annihilate and nucleate, where $\varepsilon = \left(I_o/I_{th}\right) - 1$, I_o is the incident intensity, I_{th} is the intensity at the threshold, *C* is a coefficient of order of unity, and κ is the decay rate of the optical field. To investigate the influence of transverse mode spacing $\Delta\nu_T$, we replaced the output coupler with a *R*=200 mm concave mirror. The $\Delta\nu_T$ changes from 4.3 GHz to 2.1 GHz at the same cavity length. In this case, the critical pump parameter for the onset of chaos is about ε_c=1.7. Near the lasing threshold, the dependence of pattern formations on the Fresnel number is almost identical as the previous result except that a smaller square pattern was emitted due to a larger mode size. When the pump power is increased up to $\varepsilon > 2.0$, a chaotically moving lattice defects suddently appear in the SVL pattern and the vortices annihilate and nucleate continuously, as shown in Fig. 4(a). A time-series of picture of the chaotically moving lattice defects is depicted in Fig. 4(b). The measurement of the optical spectrum shows that several different transverse-mode frequencies are simultaneously emitted around 1064 nm. The observation of the spatiotemporal instability is in agreement with the theoretical prediction.

Further increasing the cavity-Q factor by using an output coupler of *R*=50 mm with the reflectivity of 99.9%, a similar SVL pattern is emitted near the pump threshold. For the moderate values of the pump parameter power ($1 < \varepsilon < \varepsilon_c$), the transverse mode displays coexisting transverse patterns that consist of a LG-like mode on the pump region and a well-organized SVL mode in the center of the boundary, as shown in Fig. 5. The coexistence is understood from the fact that the most natural pattern of minimizing the free energy at the reflecting lateral boundaries is the formation of square vortex lattices; on the other hand, the super-high cavity Q-factor with the doughnut-shape pump profile leads to the excitation of a LG-like mode. The first evidence of coexisting patterns of different symmetries was provided in an experiment of parametrically excited surface waves [18]. The different symmetries can be due to either to selection of different wave vectors corresponding to the same wavelength or to selection of different wavelengths. The present result belongs to the former case. Recently, the coexistence of domains of different wavelengths has been observed in parametrically excited surface waves [19] and in passive nonlinear optics [20]. In laser systems, this is the first evidence of coexisting transverse patterns of different symmetry. The broadening of the power spectra shown in Fig. 4 indicates that the interaction of two patterns with different symmetries gives rise to time chaotic fluctuations. The appearance of chaotic oscillations in a coexisting transverse pattern without external periodic perturbations is of considerable interest. The two-mode route to chaotic relaxation oscillations has been observed in a microchip laser with the TEM$_{00}$ mode output in two-longitudinal-mode oscillation regime [21]. The weak cross-gain coupling among two longitudinal modes has been proposed to explain the relaxation oscillation instabilities. The chaotic oscillation of the coexisting transverse pattern can be explained with the same nonlinear gain mechanism.

四、 結論

In summary, we have demonstrated a transition from a pure LG mode to a pattern of optical vortex lattices in a large-Fresnel-number microchip laser by controlling the cavity Q-factor. Experimental results reveal that the cooperative frequency locking of nearly degenerate modes is an essential process to form stable optical vortex lattices in a class-B laser. The dependence of the SVL dynamics on the transverse-mode spacing agrees very well with the numerical analysis of the order parameter equations. The most striking observation of this investigation is that the super-high cavity Q-factor leads to the coexistence of two transverse patterns with different symmetries and the pattern-competition induced chaotic oscillations.

五、參考文獻

[1] M. C. Cross and P. C. Hohenberg, Rev. Mod. Phys. 65, 851 (1993).
[2] F. Melo, P. Umbanhowar, and H. L. Swinney, Phys. Rev. Lett. 72, 172 (1994)
[3] L. A. Lugiato (Editor), Special issue on “ *Nonlinear Optical Structures, Patterns, Chaos*”, Chaos, Solitons and Fractals, 4, 1249 (1994).
[4] T. Ackemann and W. Lange, Appl. Phys. B 72, 21 (2001).
[5] F. T. Arecchi, S. Boccaletti, P. L. Ramazza, and S. Residori, Phys. Rev. Lett., 15, 2277 (1993); K. Staliunas, G. Slekys, and C. O. Weiss, Phys. Rev. Lett. 79, 2658 (1997).
[6] K. Staliunas and C. O. Weiss, Physica D 81, 79 (1995).
[7] J. Lega, J. V. Moloney, and A. C. Newell, Phys. Rev. Lett. 73, 2978 (1994).
[8] M. Tlidi, M. Georgiou, and P. Mandel, Phys. Rev. A 48, 4605 (1993).
[9] P. Mandel, M. Georgiou, and T. Erneux, Phys. Rev. A 47, 4277 (1993)
[10] K. Staliunas and C. O. Weiss, J. Opt. Soc. Am. B 12, 1142 (1995).
[11] J. Lega, J. V. Moloney, and A. C. Newell, Physica D 83, 478 (1995)
[12] A. Barsella, C. Lepers, M. Taki, and P. Glorieux, J. Opt. B: Quantum Semiclass. Opt. 1,

64 (1999)

[13] M. Möller, B. Forsmann, and W. Lange, Chaos, Solitons and Fractals, 10, 825 (1999).

[14] K. Otsuka, P. Mandel, and E. A. Viktorov, Phys. Rev. A 56, 3226 (1997).

[15] J. J. Zayhowski, IEEE J. Quantum Electron. 26, 2052 (1990); G. J. Kintz and T. Baer, IEEE J. Quantum Electron. 26, 1457 (1990)

[16] Y. F. Chen, Y. P. Lan and S. C. Wang, Appl. Phys. B 72, 167 (2001)

[17] J. Scheuer and M. Orenstein, Science, 285, 230 (1999).

[18] S. Ciliberto and J. P. Gollub, Phys. Rev. Lett. 52, 922 (1984).

[19] B. J. Gluckman, C. B. Arnold, and J. P. Gollub, Phys. Rev. E 51, 1128 (1995); F. Melo, P. Umbanhowar, and H. L. Swinney, Phys. Rev. Lett. 75, 3838 (1995).

［20］S. Residori, P. L. Ramazza, E. Pampaloni, S. Boccaletti, and F. T. Arecchi, Phys. Rev. Lett. 76, 1063 (1996).

［21］K. Otsuka, S. L. Hwong, and B. A. Nguyen, Phys. Rev. A 61, 3815 (2000).

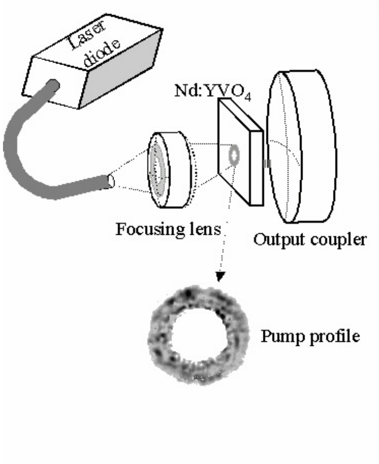

Fig. 1

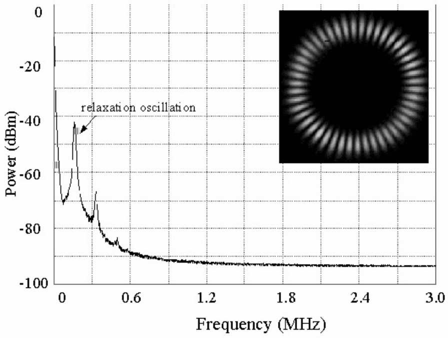
0
-20
-40
-60
-80
-100
Power (dBm)
relaxation oscillation
0
0.6
1.2
1.8
2.4
3.0
Frequency (MHz)

Fig.2

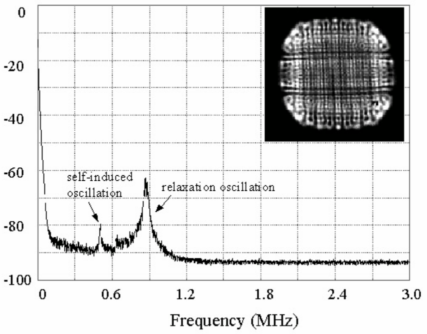
0
-20
-40
-60
-80
-100
self-induced oscillation
relaxation oscillation
0
0.6
1.2
1.8
2.4
3.0
Frequency (MHz)

Fig.3

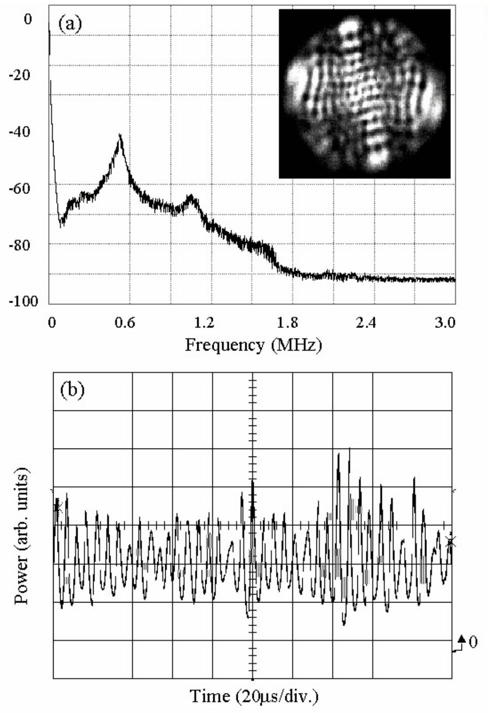
(a)
0
-20
-40
-60
-80
-100
0
0.6
1.2
1.8
2.4
3.0
Frequency (MHz)
(b)
Power (arb. units)
0
Time (20μs/div.)

Fig.4

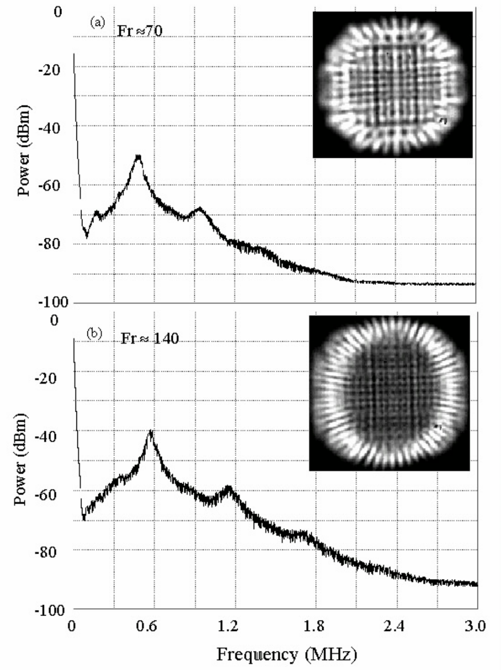
(a)
Fr≈70
Power (dBm)
0
-20
-40
-60
-80
-100
(b)
Fr≈140
Power (dBm)
0
-20
-40
-60
-80
-100
0
0.6
1.2
1.8
2.4
3.0
Frequency (MHz)

Fig.5